JOURNAL OF APPLIED ELECTROCHEMISTRY 23 (1993) 203–211

Ac impedance spectroscopy of calcium carbonate scales

R. G. COMPTON, C. A. BROWN

Physical Chemistry Laboratory, Oxford University, South Parks Road, Oxford OX1 3QZ, Great Britain

Received 6 April 1992; revised 9 July 1992

A.c. impedance spectroscopy was used to investigate the properties of a stainless steel tube, heavily scaled with calcium carbonate, and exposed to an aqueous environment. An equivalent circuit was developed to quantitatively model the observed behaviour and the results provide a possible basis for indirect monitoring of the scaling of pipes which cannot be directly viewed.

1. Introduction

A ubiquitous and highly expensive industrial problem relates to the blocking and failure of process or plant equipment and associated pipework by means of the prolonged deposition of scale particularly from hard-water supplies. The composition of this scale is often predominantly calcium carbonate (calcite, $CaCO_3$). In this paper we investigate the a.c. impedance behaviour of a stainless steel pipe internally coated with a thick layer of calcite scale with a view to assessing this experimental methodology for the indirect sensing/monitoring of scale build-up so as to permit remedy (descaling) before catastrophe (rupture).

2. Experimental details

2.1. *Instrumentation*

A.c. impedance measurements were made via a Solartron Instruments 1250 Frequency Response Analyser (Schlumberger Electronics Ltd, Farnborough, UK) used with a Solartron Instruments 1286 Electrochemical Interface employed in potentiostat mode. These were controlled by a BBC Master microcomputer which collected data subsequently displayed as an imaginary against real impedance plot using a Hewlett Packard 7470A plotter or transferred to a VAX mainframe computer for further analysis. A.c. signals of amplitude 5 mV and frequency 0.01 Hz–65 kHz were used.

2.2 *Materials and electrodes*

Measurements were made on an internally scaled stainless steel tube of internal diameter 0.540 cm and length 14.5 cm generously donated by Four Square Ltd (Basingstoke, UK). The scale was formed by passing a hot ($\sim 60\,^{\circ}C$) solution of hard water through the tube for a period of several weeks. The mean thickness of the scale, measured using a travelling microscope, was 0.083 cm. The external surface of the tube, including the end annulus, was coated in a low melting point wax, which insulated the unscaled surfaces of the metal. This was immersed to varying depths in a solution of KNO_3 supporting electrolyte (0.5 M) containing trace calcium and carbonate ions (~ 3 mM in each) to prevent the dissolution of the scale. A separate section of unscaled tubing acted as a control. The reference electrode used was a saturated calomel electrode (SCE) (K401, Radiometer, Copenhagen) and the counter electrode a graphite rod or platinum gauze sited behind a glass sinter. These electrodes were located externally to the steel tube. The d.c. potential applied to the tube was 0.0 V with respect to the reference electrode, where no net d.c. current flowed. Solutions were degassed with argon and maintained at 25 °C using a water bath.

2.3. *Modelling*

The impedance behaviour of equivalent circuits which defied ready analytical solution was found using SPICE (version 2G.5) which is a general purpose circuit simulation program for nonlinear d.c. and transient, and linear a.c. analyses. This program was run on a Norsk Data ND540 mainframe computer. Using SPICE, the required circuit was modelled by numbering the nodes where components were connected together and specifying which nodes each component was connected to, the type of component (e.g. resistor, capacitor) and the component's value. The node at which an alternating voltage was applied was also specified. The output of the program yielded the real and imaginary components, as well as magnitude, of the current at this node. Given that the voltage applied was set at zero phase, the real and imaginary components of the impedance were calculated as follows

$$Z' = -\frac{|E|\mathscr{R}(I)}{|I|^2}, \qquad Z'' = \frac{|E|\mathscr{I}(I)}{|I|^2} \tag{1}$$

where $\mathscr{R}(I)$ and $\mathscr{I}(I)$ are the real and imaginary components of the current of magnitude $|I|$ generated from SPICE.

For the modelling of transmission lines with SPICE, where the resistances and capacitances per

0021-891X

unit length are continuous, values of the components used were sufficiently small to make the circuit effectively continuous (see below).

Theoretical impedances were compared to experiment by displaying data on a $-Z''$ against Z' plot. The magnitude of the circuit components were varied to obtain the optimal fit with experiment.

3. Results and discussion

3.1. *Unscaled tube*

Experiments were first conducted using an unscaled stainless steel tube. This was partially immersed in a thermostatted electrochemical cell and electrical contact made with that part of the electrode proud of the solution surface and so unimmersed. The outside and end of the tube were insulated (see above) so that the electrode/electrolyte probed via the a.c. measurements was solely that formed at the immersed part of the inner surface of the tube. The reference and counter electrodes were located externally to the tube. The impedance plot obtained with a 0.5 M KNO_3 solution is shown in Fig. 1. This shows a 45° line at high frequencies and a near vertical line at low frequencies and an uncompensated solution resistance R_u = 24.5 Ω. Such a response can be modelled with a simple finite length open-ended (reflective) transmission line (Fig. 2) for which the following analytical equation is applicable [1,2] if it is assumed that the interfacial impedance is purely capacitative:

$$Z_{tml} = \left(\frac{R^\dagger}{2\omega C^\dagger}\right)^{1/2} \times \left(\frac{\sinh u - \sin u - j(\sinh u + \sin u)}{\cosh u - \cos u}\right) \quad (2)$$

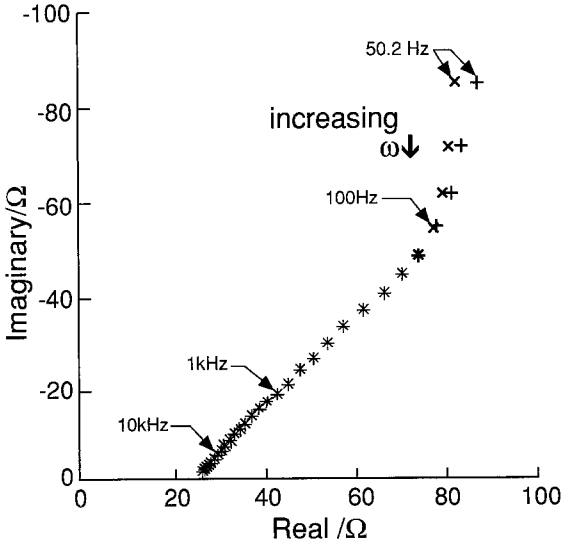

Fig. 1. Impedance plot (+) obtained from the internal surface of an unscaled tube immersed to a depth of 2 cm. This has been modelled (×) using the analytical equation for a simple reflective transmission line with $R^\dagger$ = 90 Ω cm^{-1}, $C^\dagger$ = 21 μF cm^{-1} and uncompensated solution resistance of 24.5 Ω.

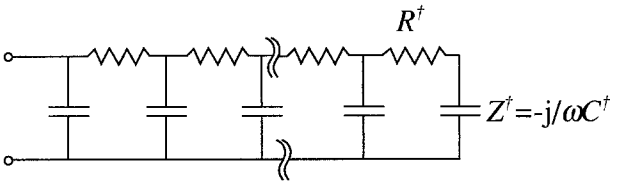

Fig. 2. A simple open-ended (reflective) finite length transmission line.

where $R^\dagger$ is the resistance and $C^\dagger$ the capacitance per unit length of transmission line of total length l, and

$$u = l(2R^\dagger C^\dagger \omega)^{1/2} \quad (3)$$

The best fit of this equation to experiment (l = 2 cm) is shown in Fig. 1 and corresponds to the parameters $R^\dagger$ = 90 Ω cm^{-1} and $C^\dagger$ = 21 μF cm^{-1}. From the internal diameter of the tube and the known molar conductivity of the solution at the ionic strength used [3] the resistance per unit length of the solution in the tube was calculated as $R^\dagger$ = 95 Ω cm^{-1} in good agreement with experiment. The low frequency data was almost, but not quite, purely capacitative i.e. the low frequency data in Fig. 1 is not quite a vertical line. This may be attributed to the surface roughness of the electrode [4–8] and can be approximately modelled with a constant phase element for which

$$Z^{-1} = A(j\omega)^\alpha \quad (4)$$

where A is a frequency independent real constant (although a more detailed treatment might allow for a fractional phase angle [9]). The exponent $\alpha = (D - 1)^{-1}$, where D ($2 < D < 3$) is the fractal dimension of the rough electrode. When D = 2 purely capacitative behaviour is obtained, corresponding to a perfectly smooth surface, whereas D = 3 gives α = 0.5, which is the limiting case for a porous electrode [2,10].

For a reflective transmission line, the value of the real impedance where the impedance plot is vertical, is given by the limit of Equation 2 where $\omega \to 0$. Expanding this equation yields

$$Z'_{\lim\omega\to 0} = \left(\frac{R^\dagger}{2\omega C^\dagger}\right)^{1/2} \frac{u}{3} = \frac{R^\dagger l}{3} \quad (5)$$

Thus at low frequencies the a.c. signal traverses the whole length of the transmission line. Consequently the validity of this model was further tested by varying the extent to which the unscaled tube was immersed in the solution. If the tube is immersed deeper into the solution, then the total resistance of the transmission line is expected to increase, as predicted by Equation 5. The impedance plots for these experiments are shown in Fig. 3 and Fig. 4 shows the fit of Equation 2 to these results, with $R^\dagger$ = 95 Ω cm^{-1} and $C^\dagger$ = 24 μF cm^{-1}. It is clear that the simple RC transmission line provides an accurate equivalent circuit for the unscaled tube in this electrode configuration.

3.2. *Scaled tube*

Experiments analogous to those described in Section

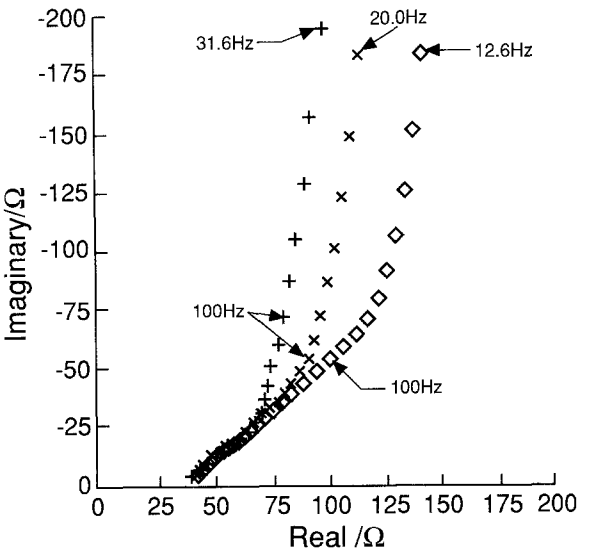

Fig. 3. Impedance plot showing the response of the unscaled tube immersed to depths of 1 cm (+), 2 cm (×) and 3 cm (◇).

3.1 were carried out on a section of scaled tube. This was 14.5 cm long and had a scale layer of mean thickness varying from 0.134 cm at the bottom to 0.064 cm at the top of the tube. Figure 5 shows impedance plots

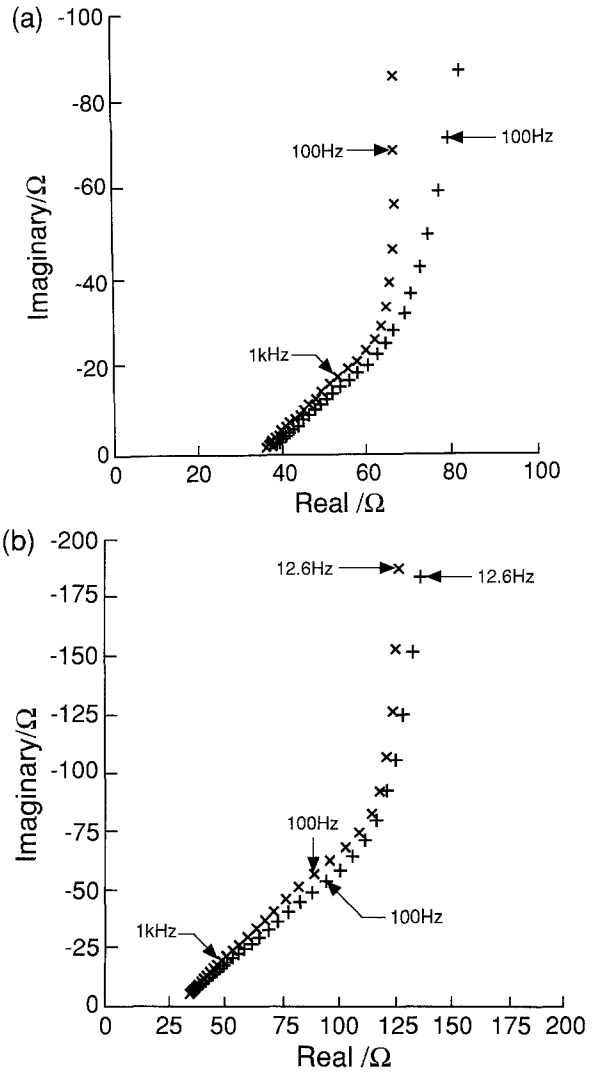

Fig. 4. Impedance plot showing the agreement between the experiment response (+) of the unscaled tube immersed to depths of (a) 1 cm and (b) 3 cm and the simple transmission line model (×) with $R^{\dagger} = 95\,\Omega\,\mathrm{cm}^{-1}$ and $C^{\dagger} = 24\,\mu\mathrm{F\,cm}^{-1}$.

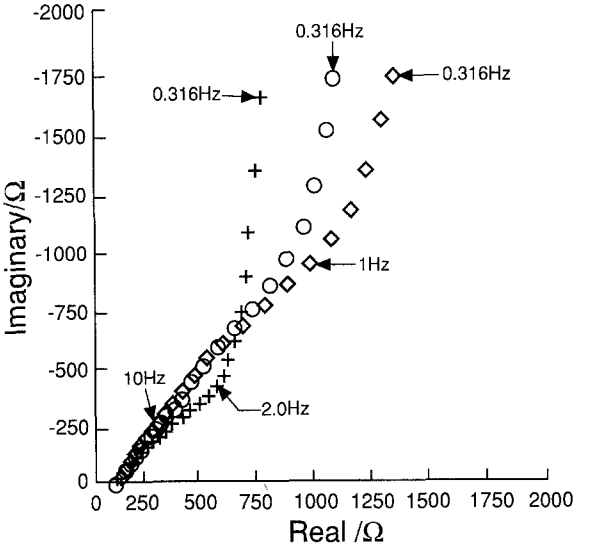

Fig. 5. Impedance plot of the scaled tube immersed to a depth of 1 cm (◇), 4 cm (○) and fully immersed (+) in a solution of 0.5 M KNO_3.

for a range of immersion depths varying from completely immersed, where the solution meniscus was just below the top of the tube to only 1 cm immersed. In each case the mean thickness of scale immersed was measured.

Candidate systems examined to model the measured behaviour included an approximate non-distributed circuit and two transmission line models as explained below.

3.2.1. Non-distributed circuit. The impedance of the non-distributed circuit, shown in Fig. 6 was derived by standard methods:

$$Z = R_u + \frac{R_s - j\omega R_s^2 C_s}{1 + (\omega R_s C_s)^2} - \frac{j}{\omega C_i} \qquad (6)$$

where R_s and C_s represent the scale resistance and capacitance, and C_i represents the capacitance of the electrode–electrolyte interface. The low frequency limit of Equation 6 is $R_u + R_s$. Fitting of this circuit to the experimental data gave reasonable fits at intermediate frequencies but at high frequencies marked disagreement was apparent (Fig. 7a and b).

3.2.2. Simple transmission line model. Next the simple *RC* transmission line (Fig. 2) which had successfully described the unscaled tube was examined and excellent agreement obtained for the fully immersed case (Fig. 8).

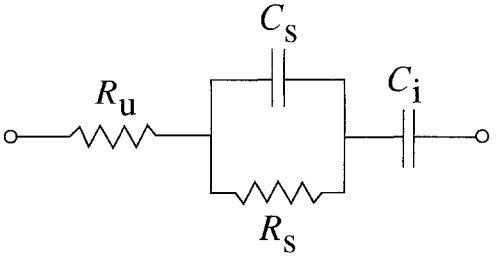

Fig. 6. Non-distributed circuit used for analysis of the data in Fig. 5 (see text).

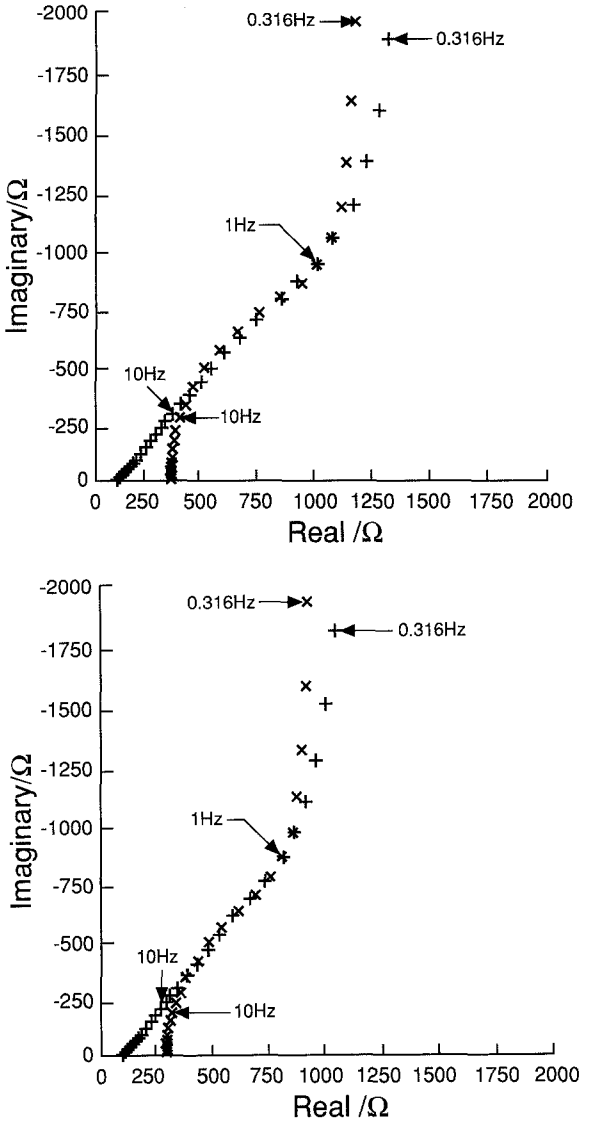

Fig. 7. Impedance plot showing the poor agreement between the impedance response of the scaled tube immersed (a) 1 cm (+) and (b) 4 cm (+) and the non distributed circuit (×), shown in Fig. 6, with: (a) $R_u = 350\,\Omega$, $R_s = 850\,\Omega$, $C_s = 98\,\mu F$ and $C_i = 277\,\mu F$; and with (b) $R_u = 300\,\Omega$, $R_s = 650\,\Omega$, $C_s = 126\,\mu F$ and $C_i = 277\,\mu F$.

Partial immersion gave reasonable qualitative agreement with the model but did not produce the expected variation with immersion. Specifically the total transmission line resistance, $R_{tml} = R^{\dagger}l$, should have been proportional to the immersion depth. Instead, as can be seen from the low frequency limit in Fig. 5 there is only a slight increase in R_{tml} with a decrease in immersion depth. Analysis showed that the low frequency (0.1–1.0 Hz) capacitance was approximately independent of immersion depth which suggested that all or most of the scale within the tube was wetted (by capillary rise), not just that immersed in the solution, and the low frequency data indicated a capacitance of 13.8 $\mu F\,cm^{-2}$ in close agreement with that of the unscaled tube.

To test this hypothesis further, the length of the scaled tube was shortened to 7 cm and the a.c. response measured with the tube completely immersed. The procedure was repeated, with the tube shortened further to 3.5 cm. The impedance behaviour

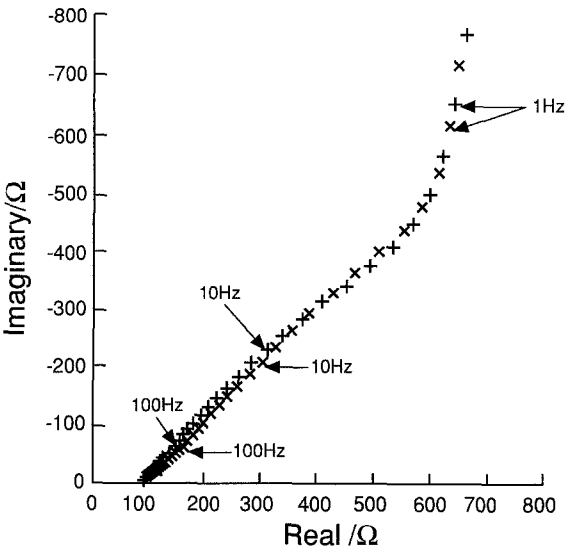

Fig. 8. Impedance plot showing agreement between data from the fully immersed scaled tube (+) and the simple transmission line model (×) with $R_u = 99\,\Omega$, $R^{\dagger} = 120\,\Omega\,cm^{-1}$ and $C^{\dagger} = 22.8\,\mu F\,cm^{-1}$.

in the three cases is shown in Fig. 9. From inspection it can be seen that the real impedance of the low frequency limit is proportional to the tube length in these experiments. The associated quantitative analysis is shown in Fig. 10, from which it is clear that the capacitance is also proportional to the length and has an average value of 15.0 $\mu F\,cm^{-2}$ (or 25.4 $\mu F\,cm^{-1}$). As can be seen from Fig. 11 the a.c. response of a fully immersed scaled tube can be modelled by a simple *RC* transmission line. This model will now be extended to rationalise the behaviour of the partially immersed tube.

3.2.3. Bipartite transmission line. The data shown in Fig. 5 demonstrated that the total transmission line resistance, R_{tml}, increased only slightly as the immersion depth decreased. This is to be expected since the resistance of the wetted scale alone, R_{so}, is greater than that for the 'parallel' combination of solution and scale R_{ss}. This was modelled using the SPICE program with

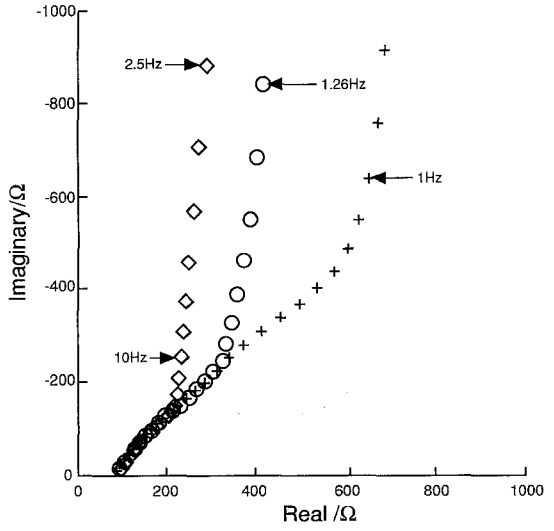

Fig. 9. Impedance plot for fully immersed scaled tubes of length 14.5 cm (+), 7 cm (×) and 3.5 cm (◇).

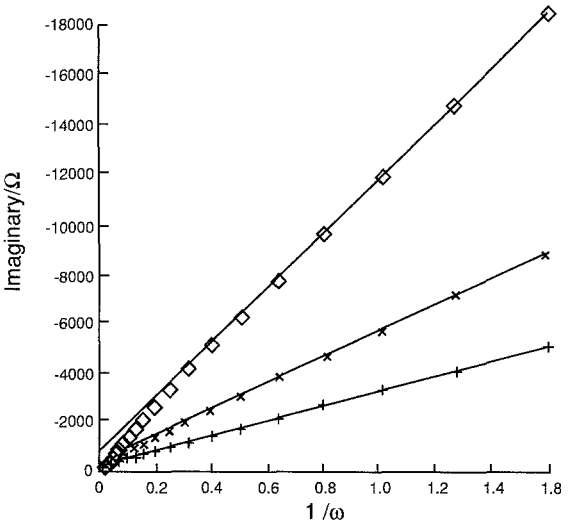

Fig. 10. Capacitance plot of the impedance data obtained for the fully immersed scaled tubes of length 14.5 cm (+), 7 cm (○) and 3.5 cm (◇). This shows that the capacitance is dependent on the immersion depth, with values of 331 μF, 192 μF and 91 μF, respectively.

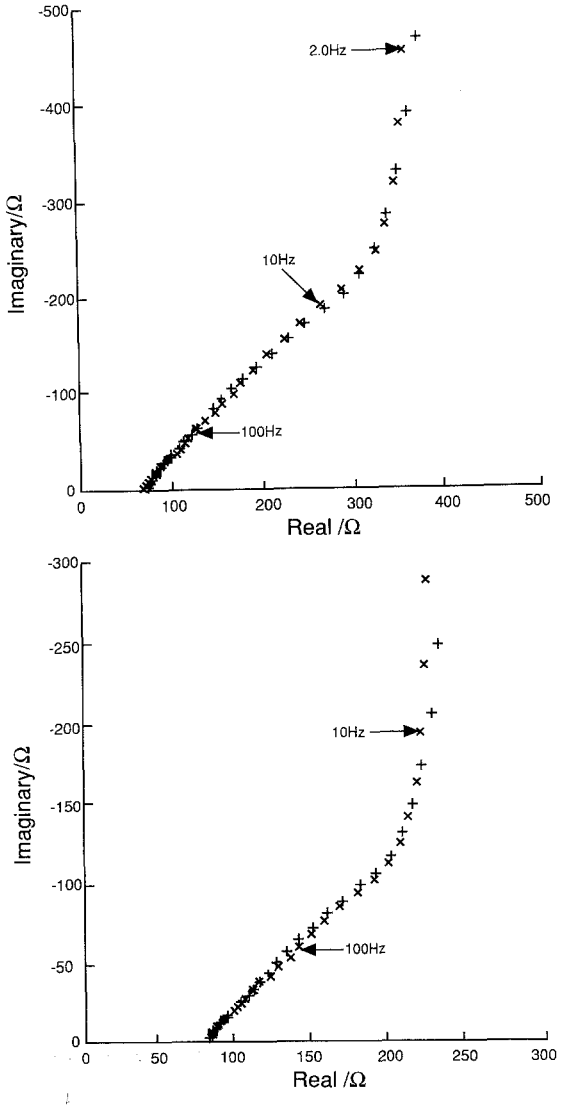

Fig. 11. Impedance plot showing the excellent agreement between data from the fully immersed scaled tube and the simple transmission line model (a) for length 7 cm (+) modelled with $R^\dagger$ = 125.7 Ω cm^{-1} and $C^\dagger$ = 27.4 μF cm^{-1} (×), and (b) for length 3.5 cm (+) modelled with $R^\dagger$ = 125.7 Ω cm and $C^\dagger$ = 26.0 μF cm^{-1} (×).

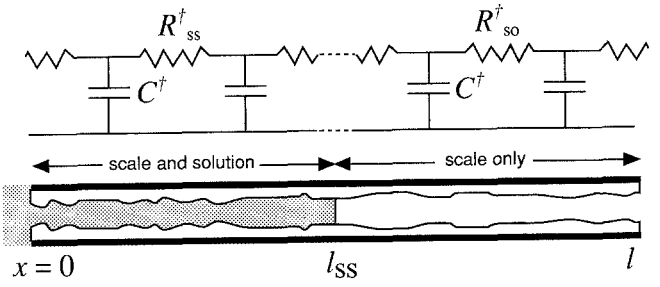

Fig. 12. Bipartite transmission line circuit.

a transmission line, but instead of a constant resistance per unit length, the value of $R^\dagger$ altered after a distance corresponding to the immersion depth (see Fig. 12). The model transmission line was constructed using 100 resistors and capacitors per centimetre. An analytical expression for the impedance of this circuit was also derived (see Appendix) and this gave perfect agreement with the SPICE program.

A mean value of $R^\dagger_{ss}$ = 124 Ω cm^{-1} was obtained from the fully immersed experimental data, as was $C^\dagger$ = 25.4 μF cm^{-1}. The values of $R^\dagger_{so}$ found to optimally fit the experimental data are given in the legends to Fig. 13 and excellent agreement is apparent, validating the bipartite transmission line model.

The scale resistance $R^\dagger_{so}$ obtained from the partial immersion experiments was compared to that estimated from the complete immersion data as follows. The thickness of the scale layer was measured at the mouth of each section of tube using a travelling microscope and hence, a mean scale thickness was calculated for each tube length used. Given the conductivity of the electrolyte [3], the resistance per unit length of the solution was calculated. Assuming the resistance of the solution and that of the scale can be treated as parallel resistors (to give the measured value of $R^\dagger_{ss}$), the resistance of the 'scale only resistor' was estimated to be 305 Ω cm^{-1} for the 14.5 cm tube and 268 Ω cm^{-1} for the 7 cm tube. This is in excellent agreement with the $R^\dagger_{so}$ values from the bipartite transmission line model, which are 300 Ω cm^{-1} and 250 Ω cm^{-1}, respectively. These separate numbers arise from a change in the mean scale thickness and explain the difference in $R^\dagger_{so}$ for the two lengths of tube.

Further evidence to confirm this model was obtained by altering the electrode configuration. The reference electrode, a silver wire electrocoated in AgBr, was sited inside the scaled tube to negate any transmission line effects. Both this and the scaled electrode were 3.5 cm long and were immersed in a solution containing 3 mM $Ca(NO_3)_2$, 3 mM K_2CO_3, $\approx$ 1 mM KBr and 0.513 M KNO_3. The electrodes were used in a two-electrode configuration so that neither the current nor potential experienced a transmission line. The impedance plot from this experiment was essentially purely capacitative.

4. Conclusions

It has been shown that the impedance of a heavily scaled tube can be modelled by a transmission line, the

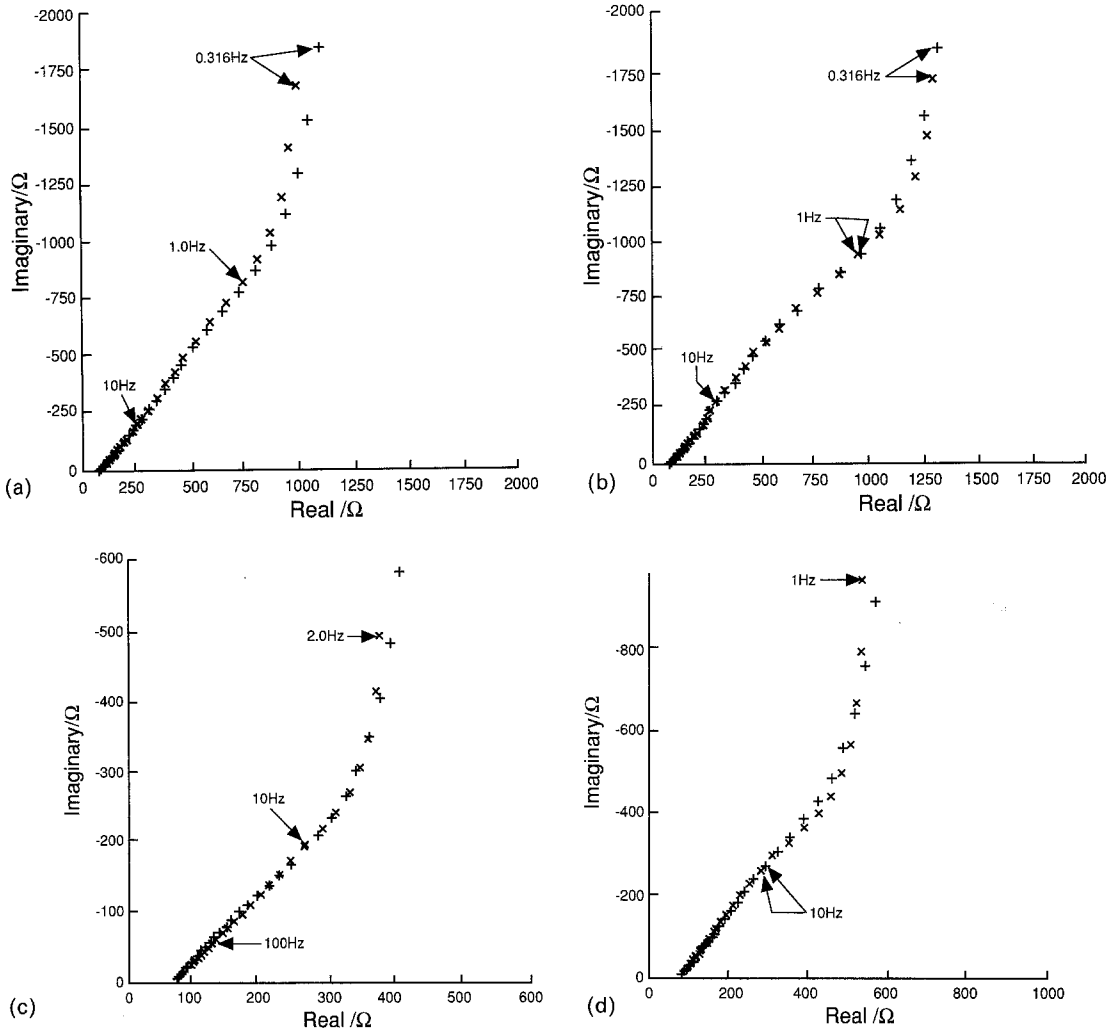

Fig. 13. Impedance plots showing the excellent agreement between experimental data (+) from scaled tubes of differing lengths immersed variously as follows and the theoretical bipartite transmission line model (×): (a) length 14.5 cm immersed to depth of 4 cm, $R_{ss}^{\dagger} = 124\,\Omega\,cm^{-1}$, $R_{so}^{\dagger} = 300\,\Omega\,cm^{-1}$ and $C^{\dagger} = 25.4\,\mu F\,cm^{-1}$; (b) length 14.5 cm immersed to depth of 1 cm, $R_{ss}^{\dagger} = 124\,\Omega\,cm^{-1}$, $R_{so}^{\dagger} = 300\,\Omega\,cm^{-1}$ and $C^{\dagger} = 25.4\,\mu F\,cm^{-1}$; (c) length 7 cm immersed to depth of 4 cm, $R_{ss}^{\dagger} = 124\,\Omega\,cm^{-1}$, $R_{so}^{\dagger} = 250\,\Omega\,cm^{-1}$ and $C^{\dagger} = 25.4\,\mu F\,cm^{-1}$; (d) length 7 cm immersed to depth of 1 cm, $R_{ss}^{\dagger} = 124\,\Omega\,cm^{-1}$, $R_{so}^{\dagger} = 250\,\Omega\,cm^{-1}$ and $C^{\dagger} = 25.4\,\mu F\,cm^{-1}$.

resistance of which is a combination of the electrolyte resistance in free solution and that in the pores of the calcium carbonate scale. The molar conductivity of 0.5 M KNO_3 in the scale pores ($\Lambda = 55.7 \pm 1.2\,S\,cm^2\,mol^{-1}$ mean value calculated from the four experiments shown in Fig. 13a–d) is rather less than that in free solution ($\Lambda = 89.24\,S\,cm^2\,mol^{-1}$ [3]). A.c. impedance techniques could therefore be used in control systems to monitor *in situ* the build up of calcium carbonate scales in pipework enabling, if necessary, shut down on attainment of critical scale levels.

References

[1] J. R. MacDonald, 'Impedance Spectroscopy', Wiley, New York (1987).
[2] R. de Levie, *Electrochim. Acta* **9** (1964) 1231.
[3] H. Falkenhagen, 'Electrolytes', Oxford University Press, Oxford (1943) p. 73.
[4] R. G. Compton, A. M. Waller, H. Block and J. Chapples, *J. Appl. Electrochem.* **20** (1990) 23.
[5] L. Nyikos and T. Pajkossy, *Electrochim. Acta* **30** (1985) 1533.
[6] *Idem, J. Electrochem. Soc.* **133** (1986) 2061.
[7] W. H. Mulder and J. H. Sluyters, *Electrochim. Acta* **33** (1988) 303.
[8] M. Keddam and H. Takenouti, *ibid.* **33** (1988) 445.
[9] R. de Levie, *J. Electroanal. Chem.* **261** (1989) 1.
[10] *Idem, Electrochim. Acta* **10** (1965) 113.

Appendix

We consider here analytically the bipartite transmission line equivalent circuit used to explain the impedance response of a scaled tube partially immersed in electrolyte. The circuit consists of an *RC* transmission line whose resistance per unit length, $R^{\dagger}$, changes at a point, $x = l_{ss}$, corresponding to the solution meniscus. Consider two infinitesimally small sections dx in the transmission line either side of the meniscus, as shown in Fig. 14. Provided small amplitude alternating voltages are used, the current response in linear and the impedance is only dependent on the frequency ω. Thus

$$0 \leqslant x \leqslant l_{ss};$$

$$dE_1 = -I_1 R_{ss}^{\dagger}\,dx \Rightarrow \frac{dE_1}{dx} + I_1 R_{ss}^{\dagger} = 0 \quad \text{(A1)}$$

$$0 \leqslant x \leqslant l_{ss};$$

$$dI_1 = -\frac{E_1}{Z^\dagger}dx \Rightarrow \frac{dI_1}{dx} + \frac{E_1}{Z^\dagger} = 0 \quad \text{(A2)}$$

and

$$l_{ss} \leqslant x \leqslant l;$$

$$dE_2 = -I_2 R^\dagger_{so}\,dx \Rightarrow \frac{dE_2}{dx} + I_2 R^\dagger_{so} = 0 \quad \text{(A3)}$$

$$l_{ss} \leqslant x \leqslant l;$$

$$dI_2 = -\frac{E_2}{Z^\dagger}dx \Rightarrow \frac{dI_2}{dx} + \frac{E_2}{Z^\dagger} = 0 \quad \text{(A4)}$$

where x is the direction along the transmission line, $R^\dagger_{ss}$ is the resistance per unit length of the first section of the transmission line (representing scale and solution), $R^\dagger_{so}$ is the resistance per unit length of the second section (scale only) and $Z^\dagger$ the impedance per unit length of the electrolyte–electrode interface.

Combining Equations A1, A2, A3, A4 gives

$$0 \leqslant x \leqslant l_{ss};\quad \frac{d^2I_1}{dx^2} - \frac{R^\dagger_{ss}}{Z^\dagger}I_1 = 0 \quad \text{(A5)}$$

$$0 \leqslant x \leqslant l_{ss};\quad \frac{d^2E_1}{dx^2} - \frac{R^\dagger_{ss}}{Z^\dagger}E_1 = 0 \quad \text{(A6)}$$

and

$$l_{ss} \leqslant x \leqslant l;\quad \frac{d^2I_2}{dx^2} - \frac{R^\dagger_{so}}{Z^\dagger}I_2 = 0 \quad \text{(A7)}$$

$$l_{ss} \leqslant x \leqslant l;\quad \frac{d^2E_2}{dx^2} - \frac{R^\dagger_{so}}{Z^\dagger}E_2 = 0 \quad \text{(A8)}$$

Solving Equation A6 yields

$$0 \leqslant x \leqslant l_{ss};$$

$$E_1(x) = A\exp\left(-x\sqrt{\frac{R^\dagger_{ss}}{Z^\dagger}}\right) + B\exp\left(+x\sqrt{\frac{R^\dagger_{ss}}{Z^\dagger}}\right) \quad \text{(A9)}$$

where A and B are defined by the boundary condition

$$x = 0;\quad A + B = E_0 \quad \text{(A10)}$$

Similarly Equation A8 gives

$$l_{ss} \leqslant x \leqslant l;$$

$$E_2(x) = A'\exp\left(-x\sqrt{\frac{R^\dagger_{so}}{Z^\dagger}}\right) + B'\exp\left(+x\sqrt{\frac{R^\dagger_{so}}{Z^\dagger}}\right) \quad \text{(A11)}$$

Applying the boundary condition at the other end of the transmission line

$$\left.\frac{dE_2}{dx}\right|_{x=0} = 0 \quad \text{(A12)}$$

together with Equation A11 yields

$$A' = B'\exp\left(2l\sqrt{\frac{R_{so}}{Z^\dagger}}\right) \quad \text{(A13)}$$

At the boundary $x = l_{ss}$ the potentials must be identical, thus

$$E_1(l_{ss}) = E_2(l_{ss}) \quad \text{(A14)}$$

as must be the current

$$\left.\frac{1}{R_{ss}}\frac{dE_1}{dx}\right|_{x=l_{ss}} = \left.\frac{1}{R_{so}}\frac{dE_2}{dx}\right|_{x=l_{ss}} \quad \text{(A15)}$$

Substituting the terms for E_1 and E_2 into these boundary conditions and solving the simultaneous equations yields the pre-exponential factor

$$B = E_0\exp\left(-l_{ss}\sqrt{\frac{R^\dagger_{ss}}{Z^\dagger}}\right)\times \frac{\left\{\begin{array}{l}(\sqrt{R^\dagger_{so}} - \sqrt{R^\dagger_{ss}})\exp\left[(2l - l_{ss})\sqrt{\frac{R^\dagger_{so}}{Z^\dagger}} - 2l_{ss}\sqrt{\frac{R^\dagger_{ss}}{Z^\dagger}}\right] \\ + (\sqrt{R^\dagger_{so}} + \sqrt{R^\dagger_{ss}})\exp\left[l_{ss}\sqrt{\frac{R^\dagger_{so}}{Z^\dagger}} - l_{ss}\sqrt{\frac{R^\dagger_{ss}}{Z^\dagger}}\right]\end{array}\right\}}{\left\{\begin{array}{l}(\sqrt{R^\dagger_{so}} - \sqrt{R^\dagger_{ss}})\exp\left[(2l - l_{ss})\sqrt{\frac{R^\dagger_{so}}{Z^\dagger}} - 2l_{ss}\sqrt{\frac{R^\dagger_{ss}}{Z^\dagger}}\right] \\ + (\sqrt{R^\dagger_{so}} + \sqrt{R^\dagger_{ss}})\exp\left[l_{ss}\sqrt{\frac{R^\dagger_{so}}{Z^\dagger}} - 2l_{ss}\sqrt{\frac{R^\dagger_{ss}}{Z^\dagger}}\right] \\ + (\sqrt{R^\dagger_{so}} - \sqrt{R^\dagger_{ss}})\exp\left[(2l - l_{ss})\sqrt{\frac{R^\dagger_{so}}{Z^\dagger}}\right] \\ + (\sqrt{R^\dagger_{so}} - \sqrt{R^\dagger_{ss}})\exp\left[l_{ss}\sqrt{\frac{R^\dagger_{so}}{Z^\dagger}}\right]\end{array}\right\}} \quad \text{(A16)}$$

The current in the first section of the transmission line is described by Equation A1 which with Equation A9 can be rewritten as

$$0 \leqslant x \leqslant l_{ss};$$

$$I(x) = \frac{1}{\sqrt{Z^\dagger R^\dagger_{ss}}}\left\{(B - E)\exp\left(-x\sqrt{\frac{R^\dagger_{ss}}{Z^\dagger}}\right) + B\exp\left(x\sqrt{\frac{R^\dagger_{ss}}{Z^\dagger}}\right)\right\} \quad \text{(A17)}$$

At the mouth of the tube the current is given by

$$I(0) = -\frac{1}{\sqrt{Z^\dagger R^\dagger_{ss}}}(2B - E_0) \quad \text{(A18)}$$

which on substituting Equation A16 yields

$$I(0) = \left(\frac{E_0}{\sqrt{Z^\dagger R_{ss}^\dagger}}\right) \times$$

$$\left\{\begin{array}{l} -(\sqrt{R_{so}^\dagger} - \sqrt{R_{ss}^\dagger}) \\ \times \exp\left[(2l - l_{ss})\sqrt{\frac{R_{so}^\dagger}{Z^\dagger}} - 2l_{ss}\sqrt{\frac{R_{ss}^\dagger}{Z^\dagger}}\right] \\ -(\sqrt{R_{so}^\dagger} + \sqrt{R_{ss}^\dagger}) \exp\left[l_{ss}\sqrt{\frac{R_{so}^\dagger}{Z^\dagger}} - 2l_{ss}\sqrt{\frac{R_{ss}^\dagger}{Z^\dagger}}\right] \\ +(\sqrt{R_{so}^\dagger} + \sqrt{R_{ss}^\dagger}) \exp\left[(2l - l_{ss})\sqrt{\frac{R_{so}^\dagger}{Z^\dagger}}\right] \\ +(\sqrt{R_{so}^\dagger} - \sqrt{R_{ss}^\dagger}) \exp\left[l_{ss}\sqrt{\frac{R_{so}^\dagger}{Z^\dagger}}\right] \end{array}\right\}$$

$$\left\{\begin{array}{l} (\sqrt{R_{so}^\dagger} - \sqrt{R_{ss}^\dagger}) \exp\left[(2l - l_{ss})\sqrt{\frac{R_{so}^\dagger}{Z^\dagger}} - 2l_{ss}\sqrt{\frac{R_{ss}^\dagger}{Z^\dagger}}\right] \\ +(\sqrt{R_{so}^\dagger} + \sqrt{R_{ss}^\dagger}) \exp\left[l_{ss}\sqrt{\frac{R_{so}^\dagger}{Z^\dagger}} - 2l_{ss}\sqrt{\frac{R_{ss}^\dagger}{Z^\dagger}}\right] \\ +(\sqrt{R_{so}^\dagger} + \sqrt{R_{ss}^\dagger}) \exp\left[(2l - l_{ss})\sqrt{\frac{R_{so}^\dagger}{Z^\dagger}}\right] \\ +(\sqrt{R_{so}^\dagger} - \sqrt{R_{ss}^\dagger}) \exp\left[l_{ss}\sqrt{\frac{R_{so}^\dagger}{Z^\dagger}}\right] \end{array}\right\} \quad \text{(A19)}$$

Hence the impedance of the bipartite transmission line is given by

$$Z_{2tml} = \sqrt{Z^\dagger R_{ss}^\dagger} \times$$

$$\left\{\begin{array}{l} (\sqrt{R_{so}^\dagger} - \sqrt{R_{ss}^\dagger}) \exp\left[(2l - l_{ss})\sqrt{\frac{R_{so}^\dagger}{Z^\dagger}} - 2l_{ss}\sqrt{\frac{R_{ss}^\dagger}{Z^\dagger}}\right] \\ +(\sqrt{R_{so}^\dagger} + \sqrt{R_{ss}^\dagger}) \exp\left[l_{ss}\sqrt{\frac{R_{so}^\dagger}{Z^\dagger}} - 2l_{ss}\sqrt{\frac{R_{ss}^\dagger}{Z^\dagger}}\right] \\ +(\sqrt{R_{so}^\dagger} + \sqrt{R_{ss}^\dagger}) \exp\left[(2l - l_{ss})\sqrt{\frac{R_{so}^\dagger}{Z^\dagger}}\right] \\ +(\sqrt{R_{so}^\dagger} + \sqrt{R_{ss}^\dagger}) \exp\left[l_{ss}\sqrt{\frac{R_{so}^\dagger}{Z^\dagger}}\right] \end{array}\right\}$$

$$\left\{\begin{array}{l} -(\sqrt{R_{so}^\dagger} - \sqrt{R_{ss}^\dagger}) \\ \times \exp\left[(2l - l_{ss})\sqrt{\frac{R_{so}^\dagger}{Z^\dagger}} - 2l_{ss}\sqrt{\frac{R_{ss}^\dagger}{Z^\dagger}}\right] \\ -(\sqrt{R_{so}^\dagger} + \sqrt{R_{ss}^\dagger}) \exp\left[l_{ss}\sqrt{\frac{R_{so}^\dagger}{Z^\dagger}} - 2l_{ss}\sqrt{\frac{R_{ss}^\dagger}{Z^\dagger}}\right] \\ +(\sqrt{R_{so}^\dagger} + \sqrt{R_{ss}^\dagger}) \exp\left[(2l - l_{ss})\sqrt{\frac{R_{so}^\dagger}{Z^\dagger}}\right] \\ +(\sqrt{R_{so}^\dagger} - \sqrt{R_{ss}^\dagger}) \exp\left[l_{ss}\sqrt{\frac{R_{so}^\dagger}{Z^\dagger}}\right] \end{array}\right\} \quad \text{(A20)}$$

If the impedance $Z^\dagger$ in Fig. 14 is replaced by a pure capacitance $C^\dagger$ then the following substitution can be made

$$Z^\dagger = +\frac{1}{j\omega C^\dagger} \quad \text{(A21)}$$

Given that

$$\sqrt{j} = \frac{1}{\sqrt{2}}(1 + j) \quad \text{(A22)}$$

and

$$\sqrt{-j} = \frac{1}{\sqrt{2}}(1 - j) \quad \text{(A23)}$$

and making the following abbreviations

$$\alpha = \left(\frac{R_{ss}^\dagger}{2\omega C^\dagger}\right)^{1/2}\left\{(2l - l_{ss})\sqrt{\frac{R_{so}^\dagger}{Z^\dagger}} - 2l_{ss}\sqrt{\frac{R_{ss}^\dagger}{Z^\dagger}}\right\} \quad \text{(A24)}$$

$$\beta = \left(\frac{R_{ss}^\dagger}{2\omega C^\dagger}\right)^{1/2}\left\{l_{ss}\sqrt{\frac{R_{so}^\dagger}{Z^\dagger}} - 2l_{ss}\sqrt{\frac{R_{ss}^\dagger}{Z^\dagger}}\right\} \quad \text{(A25)}$$

$$\gamma = \left(\frac{R_{ss}^\dagger}{2\omega C^\dagger}\right)^{1/2}(2l - l_{ss})\sqrt{\frac{R_{so}^\dagger}{Z^\dagger}} \quad \text{(A26)}$$

$$\delta = \left(\frac{R_{ss}^\dagger}{2\omega C^\dagger}\right)^{1/2} l_{ss}\sqrt{\frac{R_{so}^\dagger}{Z^\dagger}} \quad \text{(A27)}$$

Equation A20 becomes

$$Z_{2tml} = (1 - j)\left(\frac{R_{ss}^\dagger}{2\omega C^\dagger}\right) \times$$

$$\frac{\left\{\begin{array}{l} (\sqrt{R_{so}^\dagger} - \sqrt{R_{ss}^\dagger}) \exp[(1 + j)\alpha] \\ +(\sqrt{R_{so}^\dagger} - \sqrt{R_{ss}^\dagger}) \exp[(1 + j)\beta] \\ +(\sqrt{R_{so}^\dagger} - \sqrt{R_{ss}^\dagger}) \exp[(1 + j)\gamma] \\ +(\sqrt{R_{so}^\dagger} - \sqrt{R_{ss}^\dagger}) \exp[(1 + j)\delta] \end{array}\right\}}{\left\{\begin{array}{l} -(\sqrt{R_{so}^\dagger} - \sqrt{R_{ss}^\dagger}) \exp[(1 + j)\alpha] \\ -(\sqrt{R_{so}^\dagger} - \sqrt{R_{ss}^\dagger}) \exp[(1 + j)\beta] \\ +(\sqrt{R_{so}^\dagger} - \sqrt{R_{ss}^\dagger}) \exp[(1 + j)\gamma] \\ +(\sqrt{R_{so}^\dagger} - \sqrt{R_{ss}^\dagger}) \exp[(1 + j)\delta] \end{array}\right\}} \quad \text{(A28)}$$

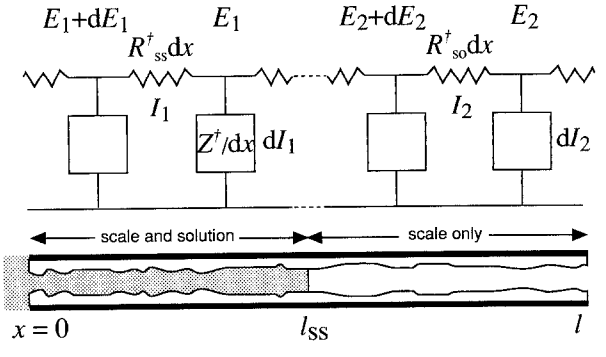

Fig. 14. Two infinitessimally small sections of the bipartite transmission line circuit, one either side of $X = l_{ss}$, which is the point corresponding to the solution meniscus.

Rewriting in trigonometric form gives

$$Z_{2tml} = (1 - j)\left(\frac{R^{\dagger}_{ss}}{2\omega C^{\dagger}}\right)^{1/2} \frac{\left\{\begin{array}{l}(\sqrt{R^{\dagger}_{so}} - \sqrt{R^{\dagger}_{ss}})e^{\alpha}\cos\alpha + (\sqrt{R^{\dagger}_{so}} + \sqrt{R^{\dagger}_{ss}})e^{\beta}\cos\beta \\ + (\sqrt{R^{\dagger}_{so}} - \sqrt{R^{\dagger}_{ss}})e^{\gamma}\cos\gamma + (\sqrt{R^{\dagger}_{so}} - \sqrt{R^{\dagger}_{ss}})e^{\delta}\cos\delta \\ + j\left[\begin{array}{l}(\sqrt{R^{\dagger}_{so}} - \sqrt{R^{\dagger}_{ss}})e^{\alpha}\sin\alpha + (\sqrt{R^{\dagger}_{so}} + \sqrt{R^{\dagger}_{ss}})e^{\beta}\sin\beta \\ + (\sqrt{R^{\dagger}_{so}} + \sqrt{R^{\dagger}_{ss}})e^{\gamma}\sin\gamma + (\sqrt{R^{\dagger}_{so}} - \sqrt{R^{\dagger}_{ss}})e^{\delta}\sin\delta\end{array}\right]\end{array}\right\}}{\left\{\begin{array}{l}-(\sqrt{R^{\dagger}_{so}} - \sqrt{R^{\dagger}_{ss}})e^{\alpha}\cos\alpha - (\sqrt{R^{\dagger}_{so}} + \sqrt{R^{\dagger}_{ss}})e^{\beta}\cos\beta \\ + (\sqrt{R^{\dagger}_{so}} + \sqrt{R^{\dagger}_{ss}})e^{\gamma}\cos\gamma + (\sqrt{R^{\dagger}_{so}} - \sqrt{R^{\dagger}_{ss}})e^{\delta}\cos\delta \\ + j\left[\begin{array}{l}-(\sqrt{R^{\dagger}_{so}} - \sqrt{R^{\dagger}_{ss}})e^{\alpha}\sin\alpha - (\sqrt{R^{\dagger}_{so}} + \sqrt{R^{\dagger}_{ss}})e^{\beta}\sin\beta \\ + (\sqrt{R^{\dagger}_{so}} + \sqrt{R^{\dagger}_{ss}})e^{\gamma}\sin\gamma + (\sqrt{R^{\dagger}_{so}} - \sqrt{R^{\dagger}_{ss}})e^{\delta}\sin\delta\end{array}\right]\end{array}\right\}} \quad \text{(A29)}$$

Multiplying the numerator and denominator by the complex conjugate of the latter and making the following abbreviations

$$\zeta_{cos1} = (\sqrt{R^{\dagger}_{so}} - \sqrt{R^{\dagger}_{ss}})e^{\alpha}\cos\alpha + (\sqrt{R^{\dagger}_{so}} + \sqrt{R^{\dagger}_{ss}})e^{\beta}\cos\beta + (\sqrt{R^{\dagger}_{so}} + \sqrt{R^{\dagger}_{ss}})e^{\gamma}\cos\gamma + (\sqrt{R^{\dagger}_{so}} - \sqrt{R^{\dagger}_{ss}})e^{\delta}\cos\delta \quad \text{(A30)}$$

$$\zeta_{cos2} = -(\sqrt{R^{\dagger}_{so}} - \sqrt{R^{\dagger}_{ss}})e^{\alpha}\cos\alpha - (\sqrt{R^{\dagger}_{so}} + \sqrt{R^{\dagger}_{ss}})e^{\beta}\cos\beta + (\sqrt{R^{\dagger}_{so}} + \sqrt{R^{\dagger}_{ss}})e^{\gamma}\cos\gamma + (\sqrt{R^{\dagger}_{so}} - \sqrt{R^{\dagger}_{ss}})e^{\delta}\cos\delta \quad \text{(A31)}$$

$$\zeta_{sin1} = (\sqrt{R^{\dagger}_{so}} - \sqrt{R^{\dagger}_{ss}})e^{\alpha}\sin\alpha + (\sqrt{R^{\dagger}_{so}} + \sqrt{R^{\dagger}_{ss}})e^{\beta}\sin\beta + (\sqrt{R^{\dagger}_{so}} + \sqrt{R^{\dagger}_{ss}})e^{\gamma}\sin\gamma + (\sqrt{R^{\dagger}_{so}} - \sqrt{R^{\dagger}_{ss}})e^{\delta}\sin\delta \quad \text{(A32)}$$

$$\zeta_{sin2} = -(\sqrt{R^{\dagger}_{so}} - \sqrt{R^{\dagger}_{ss}})e^{\alpha}\sin\alpha - (\sqrt{R^{\dagger}_{so}} + \sqrt{R^{\dagger}_{ss}})e^{\beta}\sin\beta + (\sqrt{R^{\dagger}_{so}} + \sqrt{R^{\dagger}_{ss}})e^{\gamma}\sin\gamma + (\sqrt{R^{\dagger}_{so}} - \sqrt{R^{\dagger}_{ss}})e^{\delta}\sin\delta \quad \text{(A33)}$$

Equation A29 becomes

$$Z_{2tml} = \left(\frac{R^{\dagger}_{ss}}{2\omega C^{\dagger}}\right)^{1/2} \times \frac{\left\{\begin{array}{l}(\zeta_{cos1}\zeta_{cos2} + \zeta_{sin1}\zeta_{sin2} + \zeta_{cos2}\zeta_{sin1} - \zeta_{cos1}\zeta_{sin2}) \\ + j(\zeta_{cos2}\zeta_{sin1} - \zeta_{cos1}\zeta_{sin2} - \zeta_{cos1}\zeta_{cos2} - \zeta_{sin1}\zeta_{sin2})\end{array}\right\}}{(\zeta^2_{cos2} + \zeta^2_{sin2})} \quad \text{(A34)}$$

Using Equation A34, the real and imaginary components of the bipartite transmission line circuit can be calculated for any given frequency ω.